ROTATION MINIMIZING SPHERICAL MOTIONS

B. JÜTTLER
University of Technology, Dept. of Mathematics,
Schloßgartenstr. 7, 64289 Darmstadt, Germany,
email: juettler@mathematik.tu-darmstadt.de

Abstract: In geometric design, rotation minimizing frames of space curves are used for sweep surface modeling. We give a detailed discussion of these motions within the framework of spherical kinematics. In addition we discuss their approximation by rational spline motions. The results are applied to the automatic generation of robot motions from CAD data and to the construction of sweeping surfaces.

1. Introduction

Rotation minimizing frames (RMF) of space curves are used for sweep surface modeling in computer aided design. They are characterized by the fact, that the normal plane of the curve rotates as little as possible around the tangent. In geometric design, RMF of space curves have been introduced by Klok (1986), who derives a piecewise linear approximation of the resulting sweeping surfaces. A more sophisticated approximation (consisting of surfaces of revolution) has been developed by Wang and Joe (1997). A recent manuscript by Pottmann and Wagner (1998) gives a thorough geometric discussion of RMF and sweeping surfaces.

In the present paper we discuss RMF in a kinematical setting. Given a spherical trajectory, we ask for the rotation minimizing motions (RMM) among the possible spherical motions. If the spherical trajectory is generated by the unit tangent of the curve, then the resulting motion will be the RMF of the curve.

We derive a characterization of RMM by their angular velocity. Using the kinematical mapping of spherical kinematics, it is shown that RMM correspond to special curves on Clifford–left–cylinders in elliptic 3–space. Based on quaternion calculus, we develop a scheme for approximating rotation minimizing frames with rational spline motions. We use quaternions as they are computationally efficient and particularly well suited for the construction of rational motions. The final section discusses the application of RMM to sweep surface modeling and to the automatic generation of robot motions from CAD data.

2. Rotation Minimizing Motions

Throughout this paper we consider a given curve segment $\vec{z} = \vec{z}(t)$, with the parameter $t \in [0, 1]$, on the unit sphere $S^2 \subset \mathbb{R}^3$, i.e. $\|\vec{z}\|^2 = z_1^2 + z_2^2 + z_3^2 \equiv 1$. The three components of $\vec{z}(t) = [z_1\ z_2\ z_3]^\top$ are assumed to be C^1 functions. This curve can be considered as the trajectory of the point $\vec{e}_3 = [0\ 0\ 1]^\top$ which is generated by a spherical C^1–motion, cf. (Bottema and Roth, 1979). That is, one can easily find a one–parametric system of special orthogonal matrices $U = U(t)$ which satisfy

$$\vec{z}(t) = U(t)\,\vec{e}_3 \tag{1}$$

and whose components are C^1 functions. The third column of the matrix is formed by the components of the given curve $\vec{z}(t)$. Of course, the spherical motion $U(t)$ is not uniquely determined by the condition (1). Once a motion $U(t)$ has been found, it can be composed with arbitrary rotations around the $\vec{e}_3$–axis of the moving system. Any other spherical motion $V = V(t)$ satisfying (1) can be represented as $V(t) = U(t)\,Z(t)$, with

$$Z(t) = \begin{bmatrix} \cos\phi(t) & -\sin\phi(t) & 0 \\ \sin\phi(t) & \cos\phi(t) & 0 \\ 0 & 0 & 1 \end{bmatrix}, \tag{2}$$

where the angle $\phi = \phi(t)$ is a C^1 function.
The velocity of an arbitrary point $\vec{p}_0 \in \mathbb{R}^3$ is governed by the angular velocity of the motion. Let $\vec{p}(t) = U(t)\,\vec{p}_0$ be the trajectory of $\vec{p}_0$ which is generated by the spherical motion $U(t)$. The velocity of the point on this trajectory is $\dot{\vec{p}} = \vec{\omega} \times \vec{p}$, with the angular velocity $\vec{\omega} = \vec{\omega}(t) = [\omega_1\ \omega_2\ \omega_3]^\top$ of the spherical motion $U(t)$, where $\dot{} = \frac{d}{dt}$. Resulting from $\dot{\vec{p}} = \dot{U}\,U^\top\vec{p}$, the angular velocity can easily be found from the skew–symmetric matrix $\dot{U}\,U^\top$, see (Bottema and Roth, 1979).
A short calculation leads to the angular velocity $\vec{\nu}$ of the spherical motion $V(t) = U(t)\,Z(t)$; it is the sum of the individual angular velocities,

$$\vec{\nu}(t) = \vec{\omega}(t) + \dot{\phi}\,\vec{z}(t). \tag{3}$$

Definition. The spherical motion $U = U(t)$ will be called a *rotation minimizing motion* (RMM) with the trajectory $\vec{z}(t)$, if its angular velocity is as small as possible for all $t \in [0, 1]$, that is, if it minimizes the integral

$$\int_0^1 \|\vec{\omega}(t)\|\,dt. \tag{4}$$

Due to $\|\vec{z}(t)\|^2 \equiv 1$ we get $(\vec{z}(t), \dot{\vec{z}}(t)) = 0$, hence $\dot{\vec{z}} = (\vec{z} \times \dot{\vec{z}}) \times \vec{z}$. That is, if a spherical motion $U(t)$ generates the trajectory $\vec{z}(t)$, then its angular velocity must be of the form $\vec{\omega} = (\vec{z} \times \dot{\vec{z}}) + \zeta(t)\, \vec{z}$ with an arbitrary C^0 function $\zeta(t)$. In consequence of (3) and of the above observation one has:

Proposition 1. The spherical motion $U(t)$ is a rotation minimizing motion with the trajectory $\vec{z}(t)$ if and only if its angular velocity is

$$\vec{\omega}(t) = \vec{z} \times \dot{\vec{z}}. \tag{5}$$

Proof. Assume that the spherical motion $U(t)$ satisfies (5). Consider the angular velocity (3) of the motion $V = V(t)$. In consequence of

$$\|\vec{z} \times \dot{\vec{z}} + \dot{\phi}\, \vec{z}\| \geq \|\vec{z} \times \dot{\vec{z}}\| \quad \text{we have} \quad \int_0^1 \|\vec{\nu}\|\, dt \geq \int_0^1 \|\vec{\omega}\|\, dt, \tag{6}$$

where '=' holds if and only if $\dot{\phi} \equiv 0$, as ϕ and $\vec{z}$ were assumed to be C^1 functions. This proves the assertion. □

Corollary 2. The rotation minimizing motion $U(t)$ with the trajectory $\vec{z}(t)$ does not depend on the choice of the parameterization of the given spherical curve $\vec{z}(t)$.

Proof. Consider a regular C^1 parameter transformation $t = t(s)$ of the given spherical curve $\vec{z}(t)$. Let $' = \frac{d}{ds}$. The angular velocity $\vec{\omega}^{\,*}$ with respect to the new parameter s is $\vec{\omega}^{\,*} = t'(s)\, \vec{\omega} = t'(s)\, \vec{z} \times \dot{\vec{z}} = \vec{z} \times \vec{z}\,'$. Hence, the RMM which is associated with the given spherical curve $\vec{z}(t)$ is invariant with respect to regular C^1 parameter transformations. □

3. Quaternion representation of RMM

Unit quaternions can be used in order to describe rotations, see (Bottema and Roth, 1979). For any rotation matrix U one may find a unit quaternion $Q = (q_0, q_1, q_2, q_3)$ such that the equation $U\vec{p}_0 = Q * \vec{p}_0 * \tilde{Q}$ holds for all vectors $\vec{p}_0 \in \mathbb{R}^3$, where '$*$' is the quaternion multiplication and $\tilde{Q}$ is the conjugate quaternion[1]. The components q_0 and q_1, q_2, q_3 are the real and the imaginary parts parts of the quaternion Q, respectively. Any rotation matrix U can be identified with a pair of antipodal points $\pm Q$ on the unit sphere $S^3 \subset \mathbb{R}^4$. A spherical motion $U = U(t)$ corresponds to a pair of antipodal curves $\pm Q(t) \subset S^3$.
A short calculation leads to the angular velocity of the spherical motion,

$$\vec{\omega}(t) = 2\, \dot{Q}(t) * \tilde{Q}(t), \text{ hence } \|\vec{\omega}\| = 2\|\dot{Q}\|. \tag{7}$$

[1]The vector $\vec{p}_0 = [p_{0,1}\; p_{0,2}\; p_{0,3}]^\top$ is identified with the quaternion $(0, p_{0,1}, p_{0,2}, p_{0,3})$.

By combining this equation with the result of Proposition 1 one gets a differential equation for the unit quaternion representation of the RMM which is associated with a given spherical trajectory $\vec{z}(t)$.
Using quaternion calculus we may reformulate the condition (1) as

$$\vec{z}(t) = Q(t) * \vec{e}_3 * \tilde{Q}(t), \text{ or } \vec{z}(t) * Q(t) = Q(t) * \vec{e}_3. \tag{8}$$

The latter equation forms a system of homogeneous linear equations for the components of the quaternion $Q(t)$. Hence, for any fixed parameter value $t \in [0, 1]$, the feasible quaternions (which correspond to the rotation matrices $V(t)$) form a great circular arc on $S^3 \subset \mathbb{R}^4$, as a great circular arc on S^3 is the intersection of a 2–plane through the origin of $\mathbb{R}^4$ with the unit sphere S^3.
For t varying in $[0, 1]$, the feasible unit quaternions form a 2–dimensional surface $\Phi \subset S^3$, whose parameter lines $t =$ constant are great circular arcs. (Note that the possible great circular arcs on S^3 belong to a special family of arcs on S^3. Using elliptic geometry, a characterization of this family is given below.) Let C_0 and C_1 be the great circular arcs (8) for the first point $t = 0$ and the end point $t = 1$ of the given spherical curve $\vec{z}(t)$.
Owing to (7), the integral (4) is twice the arc length of the unit quaternion curve $Q(t)$. Hence, the RMM correspond to the shortest curve on the 2–surface $\Phi \subset S^3$, which runs from a fixed point on the arc C_0 to the last arc C_1. Due to Proposition 1, this curve intersects each of the great circular arcs (8) at a right angle. This can concluded from (7) and from the fact, that the spherical motion, which is described by one of the great circular arcs (8), is a rotation around the axis $\vec{z}(t)$, i.e., its angular velocity is linearly dependent on $\vec{z}(t)$.

4. RMM in elliptic 3–space

A more geometric interpretation of RMM can be given with the help of the classical kinematic mapping of spherical kinematics, see (Müller, 1962). Any rotation matrix U is identified with the point with homogeneous coordinates λQ ($\lambda \neq 0$) in elliptic 3–space E_3. The great circular arcs on S^3 (which describe spherical motions with fixed axis) correspond simply to lines in E_3. In addition it turns out, that the great circular arcs (8) correspond to lines which are all left–parallel with respect to the so–called Clifford parallelism in elliptic 3–space, see (Müller, 1962). Hence, the 2–surface Φ can be seen as a Clifford–left–cylinder in E_3. The rotation minimizing motions $U(t)$ can be identified with the shortest curves (with respect to the elliptic metric) on the cylinder surface Φ, which run from the first generating line C_0 to the last generating line C_1 of Φ. These curves intersect the generators (8) at right angles with respect to the elliptic metric.

5. Approximate computation of RMM

Any spherical curve $\vec{z}(t)$ can be approximately converted in a so–called biarc spline curve. That is, we can always find a sequence of circular arc segments $(\vec{c}_i(t))_{i=1,\dots,n}$ (n even) on the unit sphere $S^2 \subset \mathbb{R}^3$, which approximates the original spherical curve $\vec{z}(t)$ as good as desired. The i–th segment has parameters $t \in [t_{i-1}, t_i]$, where the knots $0 = t_0 < t_1 < \dots < t_n = 1$ define a partition of the parameter interval $[0, 1]$. The circular spline curve which is obtained by collecting the segments $\vec{c}_i(t)$ is a C^1 curve. At the knots with even indices i, it matches the points $\vec{z}(t_i)$ and the first derivative vectors $\dot{\vec{z}}(t_i)$ of the original curve $\vec{z}(t)$. That is, each pair of adjacent G^1 Hermite data is interpolated with a so–called biarc. For any details concerning the construction of biarc spline curves we refer to the textbook (Nutbourne and Martin, 1988). Note that the results on planar biarcs can easily be transferred to the spherical setting via stereographic projection.

We compute the RMM for one segment of the circular spline curve. The RMM of the whole spline curve can then be found by collecting the individual segments. Consider the segment

$$\vec{c}(t) = [\ \sin(\psi)\cos(t\phi) \quad \sin(\psi)\sin(t\phi) \quad \cos(\psi)\ ]^\top, \quad t \in [0, 1], \tag{9}$$

of the parallel of latitude $\frac{\pi}{2} - \psi$ on the unit sphere S^2, where ϕ is the total angle of the arc segment. By changing coordinate systems, any circular arc segment on S^2 can be described in the above standard representation with suitable angles ψ and ϕ.

The RMM which is associated with (9) can be computed explicitly. Its quaternion representation is given by $Q(t) = Q_1(t) * Q_2(t)$ with

$$Q_1(t) = \left(\cos\tfrac{t\phi}{2}\cos\tfrac{\psi}{2},\ -\sin\tfrac{t\phi}{2}\sin\tfrac{\psi}{2},\ \cos\tfrac{t\phi}{2}\sin\tfrac{\psi}{2},\ \cos\tfrac{\psi}{2}\sin\tfrac{t\phi}{2}\right),$$

$$Q_2(t) = \left(\cos\tfrac{t\phi\ \cos\psi+\rho}{2}, 0, 0, -\sin\tfrac{t\phi\ \cos\psi+\rho}{2}\right). \tag{10}$$

The constant angle ρ specifies the initial position of the moving system. From (7) and (10) one gets the angular velocity

$$\vec{\omega} = [-\cos(t\phi)\,\phi\,\sin\psi\,\cos\psi \quad -\sin(t\phi)\,\phi\,\sin\psi\,\cos\psi \quad -\phi\,\cos^2\psi + \phi]^\top \tag{11}$$

which satisfies the condition $\vec{\omega} = \vec{c}\times\dot{\vec{c}}$ of Proposition 1. The spherical motion $Q(t)$ is spherical trochoidal motion. That is, the fixed and the moving axode of the motion are circular cones.

6. Rational approximations

Rational approximations of RMM are useful for applications in geometric design, cf. next section. We want to approximate the spherical motion

$Q(t) = Q_1(t) * Q_2(t)$ with a so-called rational motion, where all trajectories are rational curves, see (Jüttler and Wagner, 1996; Wagner and Ravani, 1997). As a major advantage of rational motions, they are compatible with the standard curve and surface representations of CAD systems.
A rational representation of a spherical motion can simply be constructed from the unit quaternion curve

$$Q(t) = \frac{1}{\|R(t)\|} R(t) \quad \text{with} \quad \|R\| = \sqrt{r_0^2 + r_1^2 + r_2^2 + r_3^2}, \qquad (12)$$

by choosing the the components of the quaternion $R = (r_0, r_1, r_2, r_3)$ as polynomials. The rotation matrix $U(t)$ of the corresponding spherical motion can easily be computed from $U\vec{x}_0 = Q * \vec{x}_0 * \tilde{Q}$, see (Bottema and Roth, 1979; Jüttler and Wagner, 1996). Its components are quadratic rational functions of the components of the quaternion R.
Firstly we consider the spherical motion $U_1(t)$ which is described by the unit quaternion curve $Q_1(t)$. A rational quadratic approximation to U_1 can be found by choosing the linear quaternion curve

$$R_1(t) = (1-t)\, B_{1,0} + t\, B_{1,1} \qquad (13)$$

with the quaternions

$$B_{1,0} = w_0\, Q_1(0) = w_0 \left(\cos\tfrac{\psi}{2},\ 0,\ \sin\tfrac{\psi}{2},\ 0\right) \quad \text{and}$$
$$B_{1,1} = w_1\, Q_1(1) = w_1 \left(\cos\tfrac{\phi}{2}\cos\tfrac{\psi}{2},\ -\sin\tfrac{\phi}{2}\sin\tfrac{\psi}{2},\ \cos\tfrac{\phi}{2}\sin\tfrac{\psi}{2},\ \sin\tfrac{\phi}{2}\cos\tfrac{\psi}{2}\right).$$

The positive weights $w_0, w_1 \in \mathbb{R}$ can be chosen arbitrarily, for instance $w_0 = w_1 = 1$. The quadratic rational motion which is obtained from the linear quaternion curve (13) describes exactly the same spherical motion as $Q_1(t)$, but with a new parameterization. That is, we have $Q_1(\tau(t)) = R_1(t)/\|R_1(t)\|$, where $\tau(t)$ is a monotonically increasing reparameterization function with $\tau(0) = 0$ and $\tau(1) = 1$. This is due to the fact that $Q_1(t)$ is a great circular arc on $S^3 \subset \mathbb{R}^4$; it describes a uniform rotation with constant axis.
Similarly we could find a quadratic rational representation for the second spherical motion $Q_2(t)$. This would produce an exact representation $R_2(t)$ of this motion with another reparameterization function $\bar{\tau}(t)$, i.e., $Q_2(\bar{\tau}(t)) = R_2(t)/\|R_2(t)\|$. Hence, the composition $R(t) = R_1(t) * R_2(t)$ is *not* the original motion $Q(t)$, as the reparameterization functions $\tau(t)$ and $\bar{\tau}(t)$ are generally different. That is, in general we are unable to find an exact rational representation for $Q(t)$.
As a theoretical result, an exact rational representation of $Q(t)$ can be found if and only if $\cos\psi$ is rational. This, however, may lead to rational motions of a rather high degree which are not suitable for applications.

In order to bypass this difficulty, we propose the following approximate solution. Let $R_1(t)$ as in (13), and let $R_2(t)$ be the quadratic quaternion curve

$$R_2(t) = (1-t)^2\, B_{2,0} + 2t(1-t)\, B_{2,1} + t^2 B_{2,2} \tag{14}$$

with the quaternions[2]

$$\begin{aligned}
B_{2,0} &= w_0\, Q_2(0) = w_0\,(1,\,0,\,0,\,0)\,,\\
B_{2,1} &= \tfrac{1}{2}\sin\tfrac{\phi}{2}\cos\psi\left((w_0 + w_1\,\cos\tfrac{\phi\cos\psi}{2})/\sin\tfrac{\phi\cos\psi}{2},\,0,0,-w_1\right),\\
B_{2,2} &= w_1 Q_2(1) = w_1\,\left(\cos\tfrac{\phi\cos(\psi)}{2},\,0,\,0,\,-\sin\tfrac{\phi\cos\psi}{2}\right)
\end{aligned} \tag{15}$$

This leads to a rational spherical motion of degree 4 which approximates the spherical motion $Q_2(t)$. The resulting spherical motion which is obtained from the quaternion curve $R(t) = R_1(t) * R_2(t)$ has the following properties.

1.) It is a rational spherical motion of degree 6 which approximates the RMM $Q(t) = Q_1(t) * Q_2(t)$. It satisfies approximately the condition of Proposition 1. That is, for each t, the angular velocity is almost perpendicular to $\vec{c}(t)$.

2.) The trajectory of the $\vec{e}_3$ is the spherical circle $\vec{c}(t)$, but it is now traced with the rational parameterization

$$\vec{c}^*(t) = \frac{(1-t)^2 r_0\,\vec{b}_0 + 2t(1-t)r_1\,\vec{b}_1 + t^2 r_2\,\vec{b}_2}{(1-t)^2 r_0 + 2t(1-t)r_1 + t^2 r_2} \tag{16}$$

where

$$\begin{gathered}
\vec{b}_0 = \begin{bmatrix} \sin\psi \\ 0 \\ \cos\psi \end{bmatrix},\ \vec{b}_1 = \begin{bmatrix} \sin\psi \\ \tan\frac{\phi}{2}\sin\psi \\ \cos\psi \end{bmatrix},\ \vec{b}_2 = \begin{bmatrix} \sin\psi\cos\phi \\ \sin\psi\sin\phi \\ \cos\psi \end{bmatrix},\\
\text{and}\quad r_0 = w_0^2,\quad r_1 = w_0 w_1\cos\tfrac{\phi}{2},\quad r_2 = w_2^2.
\end{gathered} \tag{17}$$

In addition, the end positions $t = 0, t = 1$ of $R(t)$ and $Q(t)$ are identical, as

$$R(0) = w_0^2\, Q(0) \quad \text{and} \quad R(1) = w_1^2\, Q(1). \tag{18}$$

3.) For $t = 0$ and $t = 1$, the angular velocity of $R(t)$ is perpendicular to $\vec{c}(t)$. Thus, the angular velocity at the segment end points has the exact value, as derived in Proposition 1.

If the weights w_0 and w_1 are already given (this is the case in the application of section 7.1), then the last two conditions leave one degree of freedom for

[2] These formulas are valid for $\rho = 0$ only. The coefficients for arbitrary ρ are obtained by multiplying the above quaternions with $(\cos\frac{\rho}{2},\,0,\,0,\,-\sin\frac{\rho}{2})$.

choosing the coefficients of (14). We have fixed this parameter such that the heuristic conditions $w_0 = \|R_1(0)\| = \|R_2(0)\|$ and $w_1 = \|R_1(1)\| = \|R_2(1)\|$ are fulfilled. The accuracy of the resulting rational approximation $R(t) = R_1(t) * R_2(t)$ to $Q(t) = Q_1(t) * Q_2(t)$ should be sufficient for most applications; it can be improved by increasing the number of segments of the biarc spline which approximates the given spherical trajectory $\vec{z}(t)$, cf. Section 5.

7. Applications and Examples

Finally we outline two applications of rotation minimizing motions.

7.1. ROTATION MINIMIZING FRAMES FOR SPACE CURVES

Consider a spatial curve $\vec{s} = \vec{s}(t)$. Its hodograph (also called the spherical indicatrix of tangents) is formed by the unit tangent vectors $\vec{z}(t) = \dot{\vec{s}}(t)/\|\dot{\vec{s}}(t)\|$. Let $U(t)$ be the associated RMM as defined in Section 2. The spatial motion which is described by the mapping

$$\vec{p}_0 \mapsto \vec{p}(t) = \vec{s}(t) + U(t)\,\vec{p}_0 \tag{19}$$

is called the rotation minimizing frame (RMF) of the given space curve, see also Section 1. This frame is used for modelling sweep surfaces in geometric design applications. According to Corollary 2, its definition is independent of the parameterization of the given space curve. In order to find a rational approximation to the RMF, we proceed in two steps.

1.) Firstly we convert the given curve $\vec{s}(t)$ approximately into a new curve $\vec{s}^*(t)$, whose hodograph $\vec{z}^*(t) = \dot{\vec{s}}^*(t)/\|\dot{\vec{s}}^*(t)\|$ is a sequence of circular arcs. This can be done by constructing a sequence of so–called Pythagorean–hodograph (PH) cubics (Farouki and Sakkalis, 1994) via interpolation of G^1 Hermite data (points + tangents) sampled from the original curve. The details of such a procedure have been described by Wagner and Ravani (1997). The hodograph $\vec{z}^*(t)$ is a C^0 circular spline curve on the unit sphere.In addition to the results in (Wagner and Ravani, 1997) it can be shown, that it is possible to convert the given space curve $\vec{s}(t)$ into a PH cubic spline curve with any desired accuracy, provided that it has non–vanishing curvature everywhere. The proof of this fact will be presented elsewhere.

2.) Secondly we construct – for each circular arc – a rational approximation of the RMM as described in the previous section. Note that the overall RMF of $\vec{s}^*(t)$ is a C^0 motion in general, because the hodograph $\vec{z}^*(t)$ is not guaranteed to be tangent continuous. Nevertheless, the trajectories of points travelling in the normal plane of $\vec{s}^*(t)$ are tangent continuous,

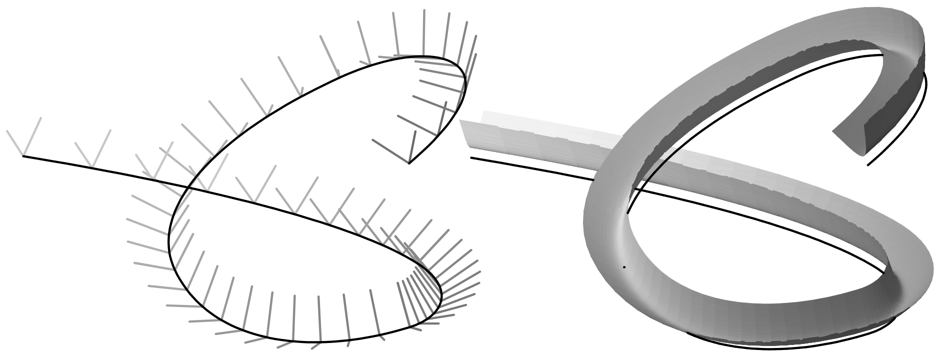

Figure 1. RMF of a space curve (left) and sweeping surface (right).

because the angular velocity of the RMF is always orthogonal to the tangent of the curve, cf. Proposition 1. Owing to their property 3.) (Section 6), the rational approximation preserves this order of continuity.

The rational approximation of the RMF can be used in order to find rational (i.e., NURBS) representations of sweeping surfaces which are generated by moving profile surfaces. The space curve $\vec{s}^*(t)$ is called the spine curve. As an advantage over the method of Wang and Joe (1997) who use a circular spline, in our method the spine curve can be a true space curve. This is helpful in order to keep the number of segments relatively small.
An example is depicted in Figure 1. The spine curve (in black) is a PH cubic spline curve with 5 segments. The left figure shows the RMF; it is visualized by the unit vectors $U(t)\,\vec{e}_1$ and $U(t)\,\vec{e}_2$ which span the normal plane of the curve. An example of a sweeping surface has been plotted on the right–hand side. It is a NURB spline surface of degree $(9,3)$ with five segments. In order to illustrate the accuracy of the rational approximation to the RMM, Figure 2 shows the angle between the real angular velocity and the curve tangent for one segment of the PH cubic spline curve. Ideally, these vectors would always be perpendicular, according to Proposition 1. For the rational approximation (where $\phi = 94.7°$ and $\psi = 81.3°$), the angle varies between $89.966°$ and $90.026°$. Hence, there is very little deviation from the RMM.

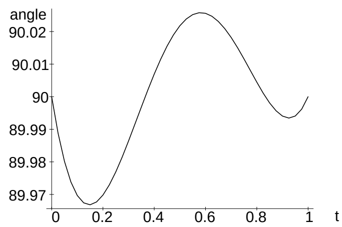

Figure 2. Plot of $\angle(\vec{z}, \vec{\omega})$.

7.2. GENERATING ROBOT TRAJECTORIES FROM CAD DATA

In order to automatize the process of robot programming, a forthcoming task will be the direct use of CAD data, as far as this is possible. For

instance, such data can be used in order to specify the path of the tool center point of the robot. However, data from CAD systems usually does not contain any information about the orientation of the end effector.
In many applications, the direction of the tool vector is determined by certain process requirements. For example, in spraying applications the spray gun should be perpendicular to the surface of the workpiece, in order to make the spraying as uniform as possible. This leaves one degree of freedom for the orientation of the end–effector.
As a natural solution, one should use rotation minimizing motions in order to design the robot motion. This solution can be found with the help of the methods from Sections 5 and 6. As the result we get a rational spline motion of the end effector with the minimum angular velocity. Rational spline motions are suitable for robot control. They are being used successfully within a commercial environment (Horsch and Jüttler, 1998).
An example is shown in Figure 3. The prescribed directions of the tool vector are represented by the dotted lines; they are perpendicular to the trajectory of the tool center point (solid curve). The RMM of the end effector is visualized by the moving box.

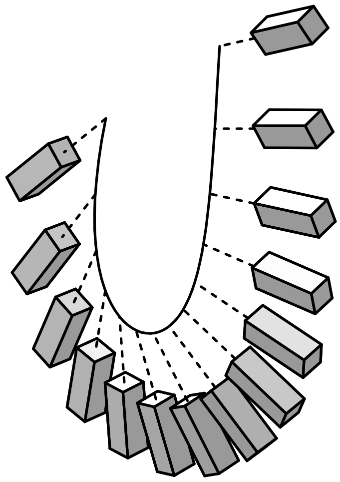
Figure 3. Rotation minimizing motion.

References

Bottema, O., and Roth, B. (1979), *Theoretical kinematics*, North–Holland, Amsterdam.
Farouki, R.T., and Sakkalis, T. (1994), Pythagorean-hodograph space curves, Adv. in Comput. Math., **vol. 2**, pp. 41-66.
Horsch, Th., and Jüttler, B. (1998), Cartesian spline interpolation for industrial robots, Comput.–Aided. Design, in press.
Jüttler, B., and Wagner, M.G. (1996), Computer Aided Design with Spatial Rational B–Spline Motions, ASME J. of Mech. Design, **vol. 118**, pp. 193–201.
Klok, F. (1986), Two moving coordinate frames for sweeping along a 3D trajectory, Comput. Aided Geom. Design, **vol. 3**, pp. 217-229.
Müller, H.R. (1962), *Sphärische Kinematik*, Deutscher Verlag der Wissenschaften, Berlin.
Nutbourne, A.W., and Martin, R.R. (1988), *Differential Geometry Applied to Curve and Surface Design. Vol. 1: Foundations*, Ellis Horwood Ltd., Chichester.
Pottmann, H., and Wagner, M.G. (1998), Contributions to Motion Based Surface Design, manuscript.
Wagner, M.G., and Ravani, B. (1997), Curves with Rational Frenet–Serret motion, Comput. Aided Geom. Design, **vol. 15**, pp. 79–101.
Wang, W., and Joe, B. (1997), Robust computation of the rotation minimizing frame for sweep surface modeling, Comput.–Aided Design, **vol. 29**, pp. 379–391.